Expanded View Figures

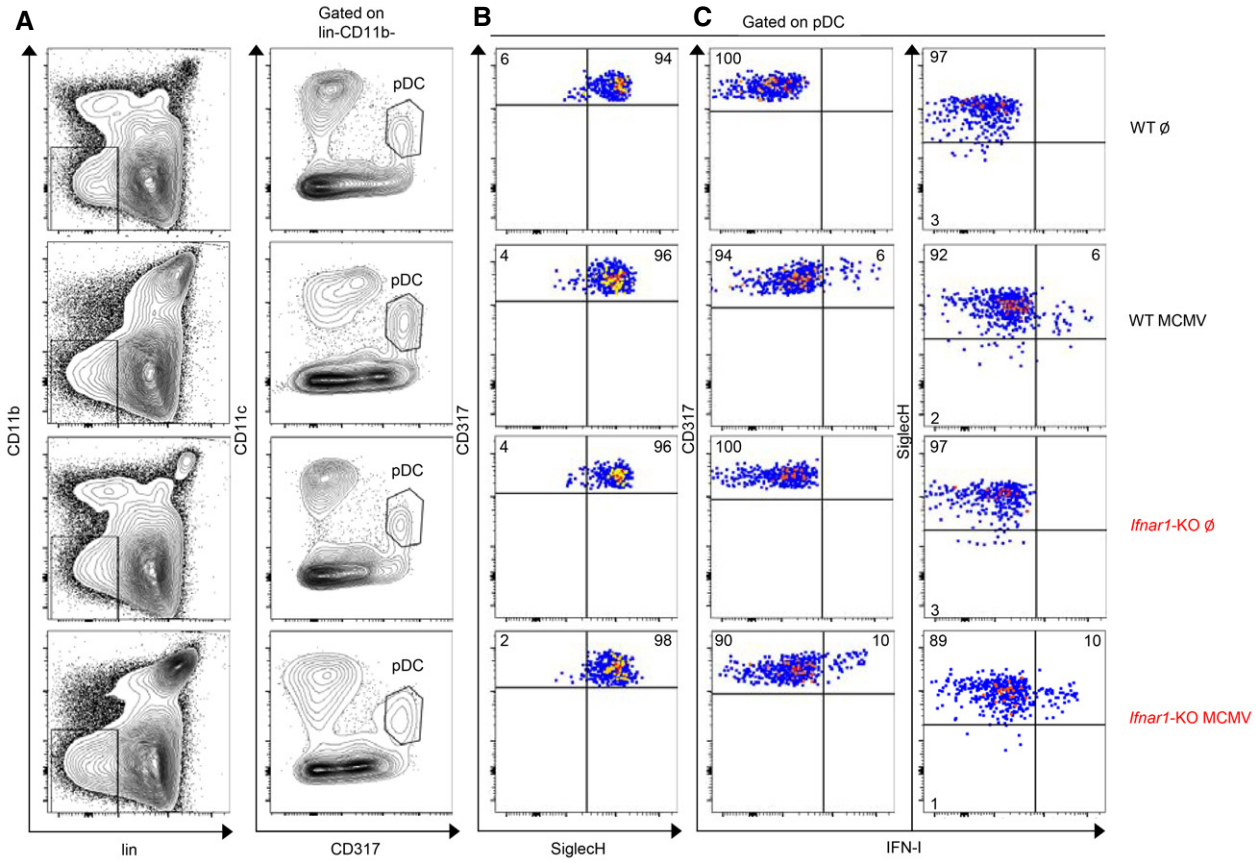

Figure EV1. Expression of CD317 and SiglecH on pDC isolated from uninfected versus MCMV-infected C57BL/6 or *Ifnar1*-KO mice.

A pDC were identified, as shown in Fig 1B, as lineage (CD3, CD19, Ly6G, NK1.1)$^-$ CD11b$^-$ CD11c$^{low/int}$ CD317^{high} cells.

B SiglecH expression was analyzed on pDC isolated from the spleen of indicated mice and gated as in (A).

C Dot plots represent IFN-I versus CD317 (left panels) or versus SiglecH (right panels) stainings in pDC isolated from indicated uninfected or MCMV-infected mice. Data are representative of two animals for uninfected mice and six animals for MCMV-infected mice from two independent experiments.

Figure EV2. Comparative gene expression profiling of sorted pDC with other cells sorted from the same mice and with an ImmGen compendium confirms specificity of gating strategy.

A Principal component analysis demonstrating overall close transcriptomic proximity between splenic pDC sorted from MBMC mice or from C57BL6 mice under steady state or MCMV infection conditions and splenic pDC sorted from uninfected C57BL/6 mice by the ImmGen consortium. The data shown were batch corrected using ComBat with a model considering each independent dataset as one batch and identity between cDC1, cDC2, RPM, and cMo across batches, but without any inference on the relationships between other cell types including pDC across batches (see Appendix Fig S1 for uncorrected data).

B Heatmap showing the expression patterns of well-known cell type-specific genes across all samples, with hierarchical clustering of cell samples (columns) and genes (rows). Note that all pDC cluster together in (A) and (B) and that each of the individual pDC samples analyzed strongly expresses the pDC gene module but none of the genes from the other cell type gene modules. Dataset numbers correspond to those indicated in the legend of panel (A).

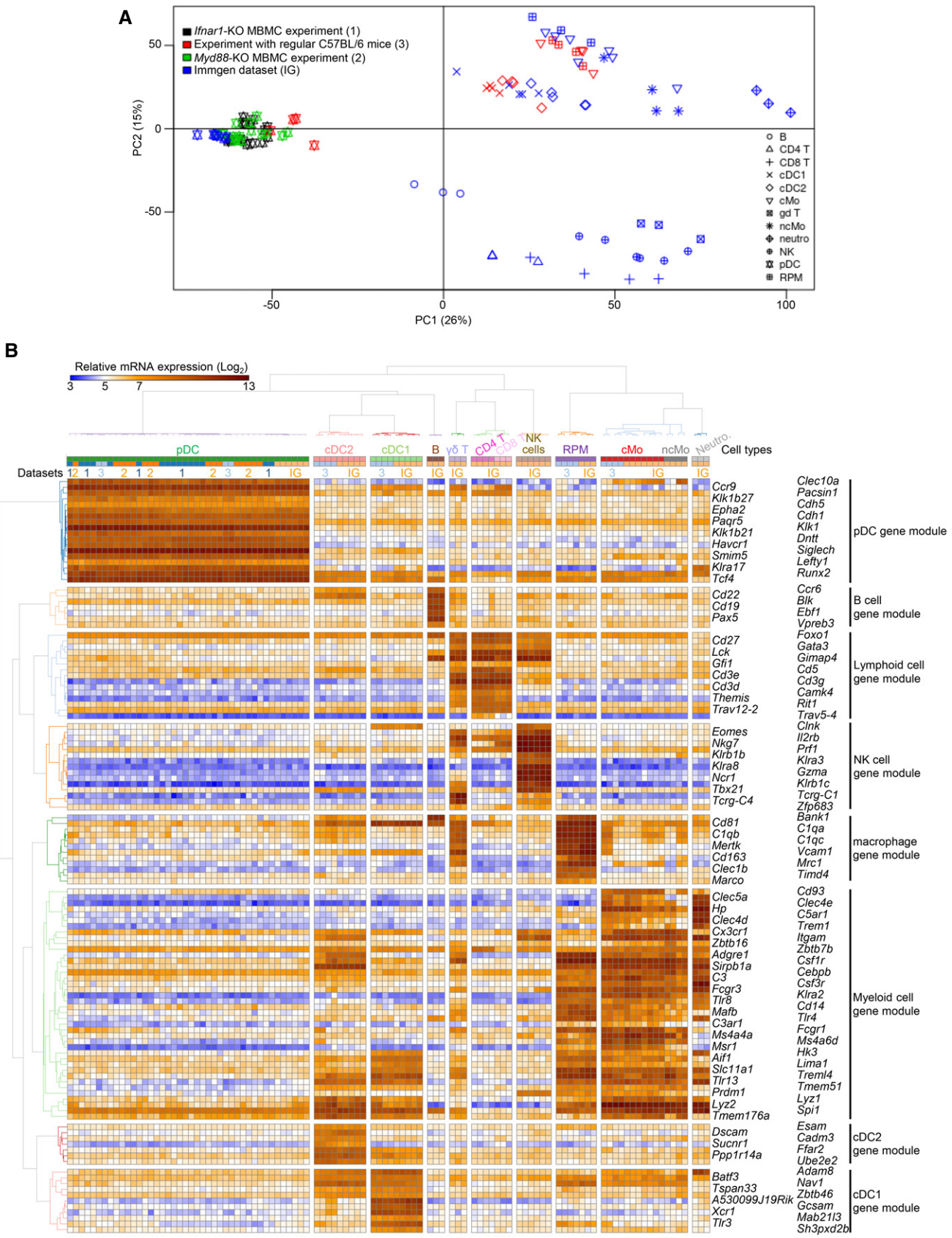

Figure EV2.

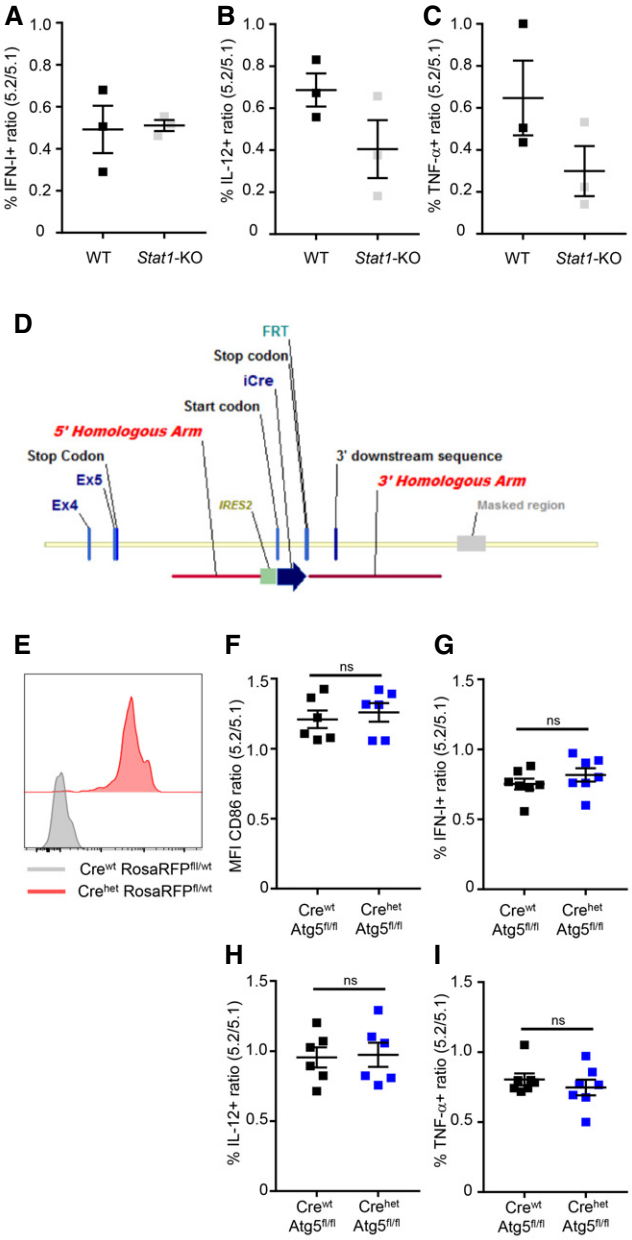

Figure EV3. STAT1 and ATG5 are dispensable for pDC cytokine production *in vivo* during MCMV infection.

A–C 5.2/5.1 ratio (mean ± SEM) of indicated cytokine-producing pDC in CTR (black) versus *Stat1*-KO (gray) MBMC mice (n = 3).

D Schematic representation of the construct used for targeting the mouse *Siglech* gene to generate the *Siglech*-iCre KI mouse strain. The cassette encoding improved Cre (*iCre*) gene was inserted in the 3′ non-coding region of *Siglech* gene. The initiation of *iCre* gene translation was under the control of internal ribosome entry site (IRES) sequences. FRT is a residual recombination site left after mouse breeding with Flipper mice expressing Flippase O in the germline, a step that was necessary to remove the *neo* selection cassette.

E *Siglech*-iCre mice were bred with *Rosa26*-LSL-RFP mice to fate-map cells in which *Siglech*-driven Cre recombination had been effective. RFP expression in splenic pDC isolated from *Siglech*-iCre^{wt} *Rosa26*-LSL-RFP$^{fl/wt}$ (gray) versus *Siglech*-iCre^{het} *Rosa26*-LSL-RFP$^{fl/wt}$ (red) is depicted. Histograms are representative of one out of ten mice tested.

F–I 5.2/5.1 ratio of CD86 MFI or of the percentages of cytokine-producing cells in pDC from *Siglech*-iCre^{wt} *Atg5*$^{fl/fl}$ (Cre^{wt} *Atg5*$^{fl/fl}$, black) or *Siglech*-iCre^{het} *Atg5*$^{fl/fl}$ (Cre^{het} *Atg5*$^{fl/fl}$, dark blue) MBMC. Data shown (mean ± SEM) are from two pooled independent experiments each with at least three mice per group. ns, not significant ($P > 0.05$); (nonparametric Mann–Whitney test).

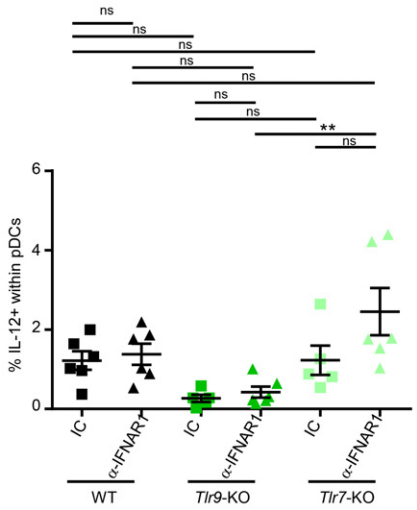

Figure EV4. During MCMV infection, the TLR9/Myd88-dependent pathway is necessary for pDC IL-12 production, irrespective of their IFN-I responsiveness.

Percentages of IL-12-producing cells within pDC of each indicated mouse strain. Black, C57BL6; green, *Tlr9*$^{-/-}$ and pale green, *Tlr7*$^{-/-}$. Mice were treated with IC (square) or blocking α-IFNAR1 mAbs (triangle). Data depicted (mean ± SEM) are from two pooled independent experiments each with two to three mice per group. ns, not significant ($P > 0.05$); **$P < 0.01$; (nonparametric Mann–Whitney test).

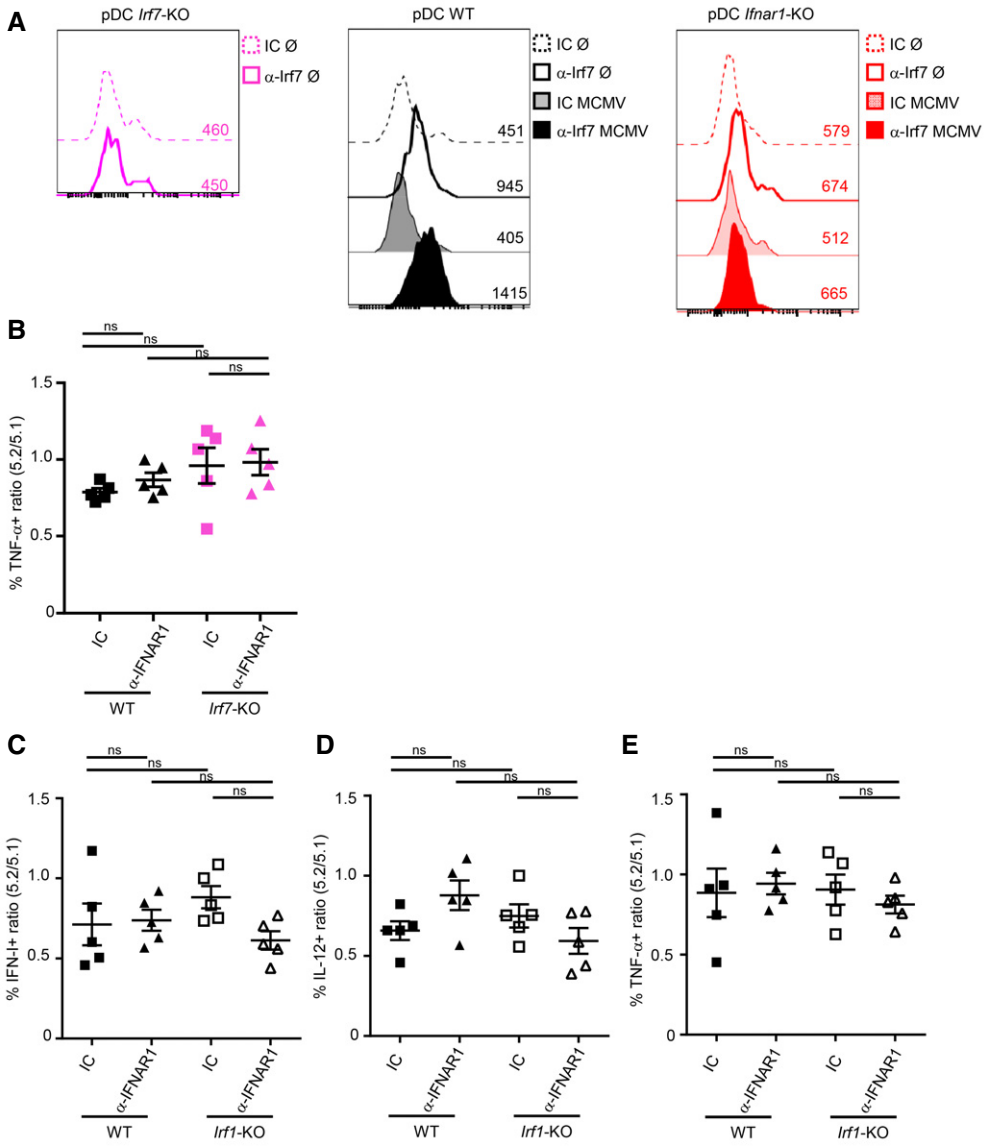

Figure EV5. IRF1 is not necessary for IFN-I production in pDC during MCMV infection, even in the absence of IFN-I-responsiveness.

A IRF7 protein expression in pDC isolated from *Irf7*$^{-/-}$ (pink, left), C57BL/6 (WT, black, middle), and *Ifnar1*$^{-/-}$ (red, right) mice. Empty histograms, uninfected mice (Ø); with bold line, IRF7 staining (a-IRF7) and dotted line, isotype control (IC) staining. Filled histograms, infected mice (MCMV); with dark color, IRF7 staining, and pale color, IC staining. For each condition, histograms are representative of one out of four to six mice from two independent experiments.

B Ratio of TNF-producing cells in 5.2^{+} versus 5.1^{+} pDC of each indicated MBMC. Black, CTR MBMC; pink, *Irf7*$^{-/-}$ TST MBMC. Mice were treated with isotype control (IC, square) or blocking α-IFNAR1 mAbs (triangle). Data shown (mean ± SEM) are from two pooled independent experiments each with two to three mice per group.

C–E Ratio of cytokine-producing cells in 5.2^{+} versus 5.1^{+} pDC of each indicated MBMC. Black, CTR MBMC; white, *Irf1*$^{-/-}$ TST MBMC. Mice were treated with isotype control (IC, square) or blocking α-IFNAR1 mAbs (triangle). Data shown (mean ± SEM) are from two pooled independent experiments each with two to three mice per group. ns, not significant; (nonparametric Kruskal–Wallis test combined with Dunn's multiple correction test) for panels (B–E).

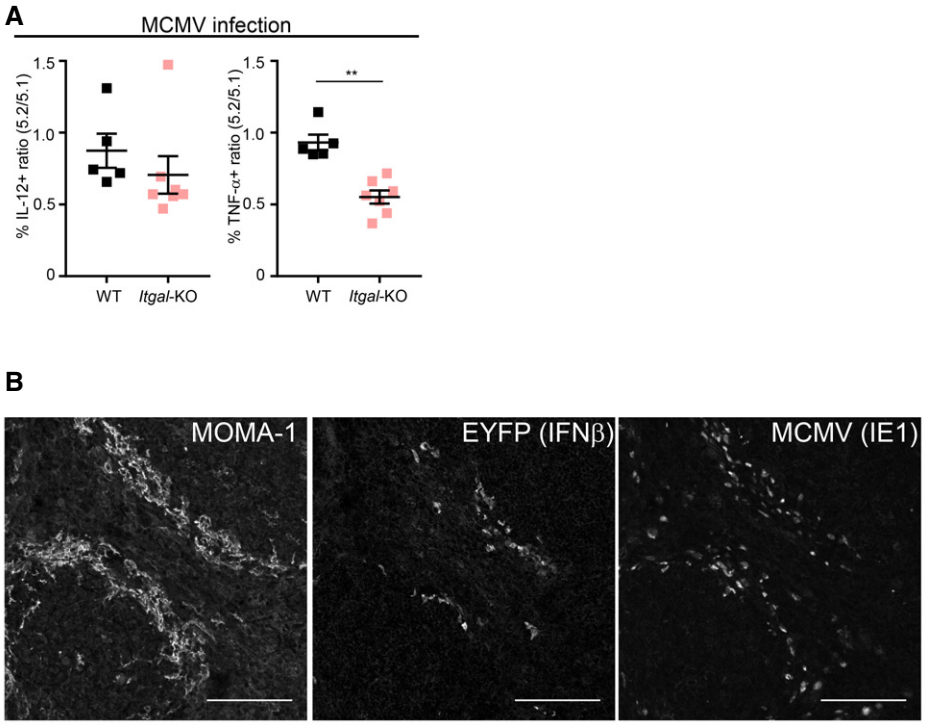

Figure EV6. LFA-1 is necessary for TNF, but not for IL-12 production in pDC during MCMV infection.

A Ratio of TNF and IL-12 production in 5.2^+ versus 5.1^+ pDC isolated from MCMV-infected MBMC of each indicated type. Black, CTR MBMC; pale pink, *Cd11a*$^{-/-}$ TST MBMC. Data shown (mean ± SEM) are from two pooled independent experiments each with three mice per group. $^{**}P < 0.01$; (nonparametric Mann–Whitney test).

B Individual color images of Fig 7D have been represented as black and white. Scale bars, 100 μm.